ENVIRONMENTAL RESEARCH
COMMUNICATIONS

LETTER • OPEN ACCESS

Quasi-biennial modulation of rapidly intensifying tropical cyclones by the western North Pacific monsoon

To cite this article: Jinjie Song *et al* 2023 *Environ. Res. Commun.* **5** 051009

Environmental Research Communications

CrossMark

OPEN ACCESS

RECEIVED
6 February 2023

REVISED
27 April 2023

ACCEPTED FOR PUBLICATION
10 May 2023

PUBLISHED
26 May 2023

LETTER

Quasi-biennial modulation of rapidly intensifying tropical cyclones by the western North Pacific monsoon

Jinjie Song[1,2], **Philip J Klotzbach**[3], **Qingyuan Liu**[1,2] and **Yihong Duan**[2,*]

[1] Nanjing Joint Institute for Atmospheric Sciences, Chinese Academy of Meteorological Sciences, Nanjing, People's Republic of China
[2] State Key Laboratory of Severe Weather, Chinese Academy of Meteorological Sciences, Beijing, People's Republic of China
[3] Department of Atmospheric Science, Colorado State University, Fort Collins, CO, United States of America
[*] Author to whom any correspondence should be addressed.

E-mail: duanyh@cma.gov.cn

Keywords: tropical cyclone, rapid intensification, western North Pacific

Supplementary material for this article is available online

Abstract

Previous publications have highlighted the relationship between several climate modes such as El Niño–Southern Oscillation and tropical cyclones (TCs) experiencing rapid intensification (RI) over the western North Pacific (WNP), particularly on a 3–7-yr timescale. This study investigates the modulation of TCs experiencing RI by the WNP monsoon on biennial timescales. There is a significant positive relationship between rapidly intensifying TC (RITC) frequency over the WNP during July–November from 1980 to 2021 and the simultaneous WNP monsoon index. After classifying different WNP monsoon years on biennial timescales, we find significantly more TCs forming over the key region from 5°–25°N, 140°–160°E during strong WNP monsoon years. Some of these TCs then move westward into the portion of the WNP that climatologically has the most RI-favorable environmental conditions. Alternatively, other TCs forming in the key region move northward and undergo RI quickly after genesis, subsequently leading to an increase in rapidly intensifying WNP TC frequency. The WNP monsoon influences rapidly intensifying TC activity predominantly through modulation of large-scale atmospheric conditions. During strong WNP monsoon years, increased low-to-mid-level humidity, low-level vorticity and upper-level divergence and decreased vertical wind shear all favor TC genesis and RI development over the key region. A strong WNP monsoon is also associated with an anomalous 850-hPa cyclone, an anomalous 200-hPa anticyclone, increased 600-hPa moisture convergence and a decrease in the magnitude of 200-hPa winds over the key region. Our study highlights that the WNP monsoon significantly modulates TC and RITC activity at distinct timescales.

1. Introduction

Tropical cyclone (TC) rapid intensification (RI) is commonly defined as a pronounced intensity increase over a short duration. Forecasting RI has posed a significant challenge in improving TC intensity prediction, mainly due to an incomplete understanding of physical mechanisms responsible for RI (DeMaria *et al* 2021). TCs that undergo RI during their lifetimes (RITCs) typically have an increased chance to attain a greater lifetime maximum intensity (LMI) than other TCs. Lee *et al* (2016) showed that RITCs account for a majority (79%) of global TCs reaching major TC intensity (LMI $\geqslant$ 96 kt; Category 3 or higher on the Saffir–Simpson Hurricane Wind Scale). Owing to their generally higher intensities, RITCs can generate devastating losses for coastal regions. For instance, Super Typhoon Haiyan (2013), an RITC over the western North Pacific (WNP), caused 6300+ fatalities and ~$2 billion US dollars in damage in the Philippines (Galvin 2014). Further investigation of RITCs is thus needed for reduction of TC-related disasters.

Given the increased focus of climate change's impacts on TCs, several studies (e.g., Wang and Zhou 2008, Fudeyasu *et al* 2018, Gao *et al* 2020, Shi *et al* 2020, Cai *et al* 2022) have investigated interannual changes in WNP RITCs. The WNP is the most TC-active basin around the globe on an annually-averaged basis (Chan 2005). It is now well accepted that El Niño–Southern Oscillation (ENSO) is the primary factor influencing the interannual variability of WNP TCs (Emanuel 2018, Lin *et al* 2020, Gao *et al* 2022). Wang and Zhou (2008) and Fudeyasu *et al* (2018) found that both the occurrence number and ratio of WNP RITCs were on average higher in El Niño years than in La Niña years. During El Niño, increased RITC activity has been linked to more TCs forming over the southeastern quadrant of the WNP. These storms have a greater opportunity to undergo RI since they often pass through the region that climatologically has the most RI-favorable conditions (Fudeyasu *et al* 2018). Shi *et al* (2020) reported that the occurrence proportion of WNP RITCs exhibited distinct features between different El Niño flavors. Higher RITC ratios were observed during July–October (November–December) for eastern (central) Pacific El Niño years.

Recently, several publications have noted other factors controlling WNP RITC variability on interannual timescales. Gao *et al* (2020) found a significant positive correlation between tropical Indian Ocean sea surface temperature (SST) anomalies and the occurrence ratio of WNP RITCs. During years with positive tropical Indian Ocean SST anomalies, both a warmer ocean and a moister mid-troposphere over the WNP enhance RITC activity, while changes in dynamical conditions played a minor role. In addition, Cai *et al* (2022) showed a lag relationship between January–March eastern Tibetan Plateau snow depth (TPSD) and WNP RITC frequency during the following July–November. Increased TPSD induced a low-level anomalous anticyclone over the subtropical eastern North Pacific through modulation of the prevailing trans-Pacific westerly jet, subsequently resulting in a negative Pacific meridional mode-like SST feature. This SST pattern further triggered a low-level anomalous anticyclonic circulation over the WNP by a Gill-type Rossby response, dynamically suppressing RITC activity.

Note that all of the aforementioned factors influencing WNP RITCs typically have a timescale of longer than two years. Various ENSO indices exhibit an oscillation with a 3–7-yr preferred timescale (Wang *et al* 2016), while the basinwide Indian Ocean SST index shows a preferred periodicity of ~4-yr (Taschetto and Ambrizzi 2012). On the other hand, there is quasi-biennial variability in the tropical troposphere, which is not fully associated with interannual changes in ENSO (Meehl 1987, Meehl and Arblaster 2002, Meehl *et al* 2003). This quasi-biennial signal has been observed over the Asia-Pacific monsoon region and is typically represented by a relatively strong monsoon followed by a relatively weak monsoon and vice versa (Meehl and Arblaster 2002, Meehl *et al* 2003).

Part of the Asia-Pacific monsoon system is the WNP monsoon over the WNP TC-active region. The WNP monsoon is characterized by a northwest-southeast oriented monsoon trough with intense precipitation, low-level southwesterlies and upper-tropospheric easterlies (Tao and Chen 1987, Murakami and Matsumoto 1994). Previous studies have found that more than 70% of WNP TC genesis events were linked to the monsoon trough, which favors TC development through providing an environment of large low-level cyclonic vorticity (Briegel and Frank 1997, Ritchie and Holland 1999, Chen *et al* 2004). On interannual timescales, Wu *et al* (2012) found a strong linkage between WNP TC activity and monsoon trough location. More (fewer) TCs formed over the southeastern quadrant of the WNP during years when the monsoon trough extended eastward (retreated westward). Moreover, Choi *et al* (2016) showed that on average, WNP TCs attained higher (lower) intensities and tended to have recurving (straight-moving) tracks in strong (weak) monsoon years.

As summarized above, the WNP monsoon has been extensively studied for its impact on TC genesis. However, few studies have investigated the influence of the WNP monsoon on interannual changes related to WNP RITCs. Furthermore, WNP monsoon variability displays two preferred timescales: one on the low-frequency ENSO timescale (~4 years) and the other on a quasi-biennial timescale (Li and Wang 2005). Here we investigate the potential timescale(s) linking WNP monsoon variability and WNP RITCs.

The remainder of the manuscript is organized as follows. Section 2 introduces the TC and environmental datasets and the analysis methods. Sections 3 and 4 discuss the temporal and spatial relationship between the WNP monsoon and RITC activity, respectively. Section 5 describes how the WNP monsoon modulates environmental changes. Section 6 concludes and summarizes.

2. Data and methods

This study examines TCs forming over the WNP during 1980–2021 that reached an LMI of tropical storm intensity or higher (1-min maximum sustained wind speed $\geqslant$ 34 kt), as derived from the Joint Typhoon Warning Center best track data as compiled in the International Best Track Archive for Climate Stewardship (IBTrACS) (v04r00, Knapp *et al* 2010). TC genesis is identified as the first instance for each TC where the intensity is at least 34 kt. TCs that form over the eastern North Pacific and then enter the WNP are excluded,

Table 1. List of strong and weak WNP monsoon years and their corresponding frequencies of TCs and RITCs.

Strong WNP monsoon			Weak WNP monsoon		
Year	N_{TC}	N_{RITC}	Year	N_{TC}	N_{RITC}
1982	17	10	1981	20	5
1984	24	10	1983	20	5
1986	18	7	1985	18	3
1990	24	7	1988	20	8
1994	28	10	1993	23	9
1996	29	12	1995	22	9
2001	22	12	1998	16	7
2007	20	9	2004	18	9
2009	18	9	2008	19	5
2011	13	8	2010	13	7
2013	22	11	2012	18	7
2016	25	12	2015	17	10
2018	22	11	2017	22	9
			2020	21	7
Mean	21.7	9.8	Mean	19.1	7.1

consistent with Fudeyasu *et al* (2018). TC best track data from 1980–2021 are usually considered to be of higher quality given the near-global coverage of geostationary satellites (Daloz and Camargo 2018). Similar to previous RI-related publications (e.g., Kaplan and DeMaria 2003, Kaplan *et al* 2010, Shu *et al* 2012, Knaff *et al* 2018), an RI event is defined as a 24-h intensity increase of at least 30 kt over water, while an RITC is a TC experiencing at least one RI event during its lifetime. A higher threshold (e.g. 40 kt or 45 kt) was applied by Li *et al* (2022) to define RI over different basins. This definition provided a more physically-based threshold and described a more reliable representation of extreme intensification events (Li *et al* 2022). The results that we display are almost unchanged if a 45-kt threshold is used to identify WNP RI events (see supplementary figures 1 and 2 for further information). We investigate RITC activity during July–November. These five months include a majority (84%) of WNP RI events occurring over the entire year (Wang and Zhou 2008, Ge *et al* 2018).

Monthly mean SST and atmospheric variables are obtained from the fifth generation European Centre for Medium-Range Weather Forecasts (ECMWF) reanalysis of the global climate (ERA5; Hersbach *et al* 2020), with a resolution of $0.25° \times 0.25°$. Monthly mean ocean subsurface temperature profiles are provided by the control member of the ECMWF Ocean Reanalysis System 5 (ORAS5; Zuo *et al*, 2019) on a $1° \times 1°$ grid. We consider six environmental factors which have been found to affect RI activity (e.g., Lin *et al* 2009, Shu *et al* 2012, Lin *et al* 2013, Fudeyasu *et al* 2018, Knaff *et al* 2018, Gao *et al* 2022), including SST, tropical cyclone heat potential (TCHP), 700–500-hPa relative humidity, 850-hPa relative vorticity, 200-hPa divergence and 850–200-hPa vertical wind shear. These factors are averaged during July–November. The results do not significantly change when 6-hourly reanalysis data are used, and the days with WNP RI occurrences are excluded (see supplementary figure 3).

Following Wang and Fan (1999), the annual WNP monsoon index (WNPMI) is calculated as:

$$\mathrm{WNPMI} = U850_{(5°-15°\mathrm{N},100°-130°\mathrm{E})} - U850_{(20°-30°\mathrm{N},110°-140°\mathrm{E})} \tag{1}$$

where $U850$ denotes the ERA5 areal-averaged zonal wind during July–November at 850 hPa. Choi *et al* (2016) defined the ten years with the highest (lowest) values as the positive (negative) WNPMI phase and then discussed the WNP monsoon's effect on interannual changes in WNP TC activity. Their study did not focus on a specific period but on a relatively wider range of periods. To highlight the monsoon-RITC relationship on biennial timescales, we employ the classification method proposed by Meehl and Arblaster (2002) and Meehl *et al* (2003). This classification method has been applied to analyze the influence of the Tropospheric Biennial Oscillation (TBO). A strong monsoon during year i is defined as:

$$\mathrm{WNPMI}_{i-1} < \mathrm{WNPMI}_{i} > \mathrm{WNPMI}_{i+1} \tag{2}$$

while a weak monsoon year is defined as:

$$\mathrm{WNPMI}_{i-1} > \mathrm{WNPMI}_{i} < \mathrm{WNPMI}_{i+1} \tag{3}$$

Table 1 displays the 13 strong monsoon years and the 14 weak monsoon years identified by equations (2) and (3).

The significance levels (p) of correlation coefficients (r) between the two series and the differences in means of the samples between strong and weak monsoon years are both estimated using a two-tailed Student's t-test. In

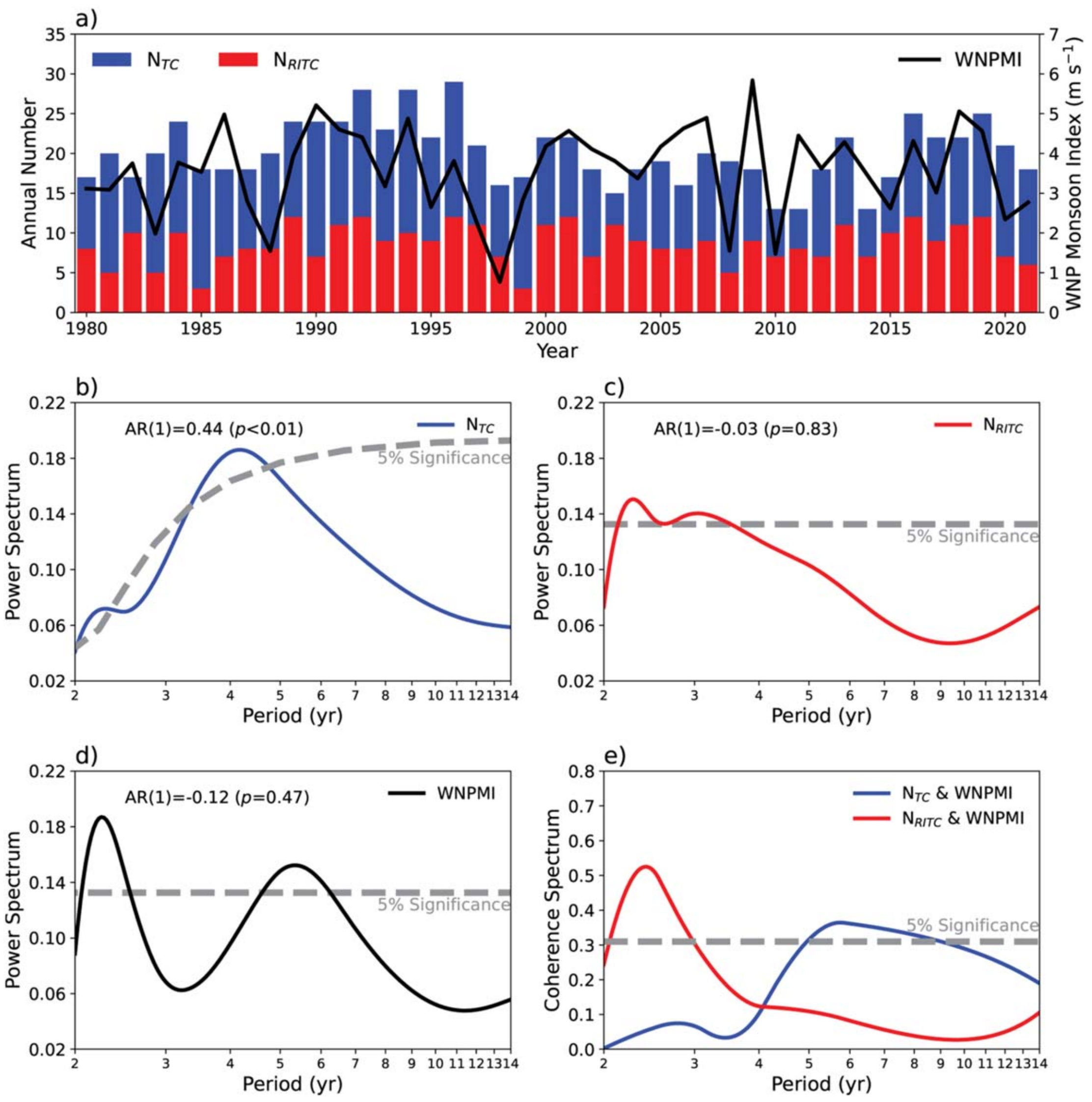

Figure 1. (a) Annual numbers of TCs and RITCs over the WNP during July–November for the period of 1980–2021, as well as the simultaneous WNPMI. (b–d) Power spectra of (b) TC and (c) RITC frequencies and (d) the WNPMI. The first order auto-correlation coefficient [AR(1)] and its significance level are given in each panel. Dashed lines denote the 0.05 significance curves based on white noise for an insignificant AR(1) or based on red noise for a significant AR(1). (e) Coherence spectra of TC frequency versus WNPMI and RITC frequency versus WNPMI. A dashed line denotes the 0.05 significance level based on an *F*-test.

evaluating statistical significance, the effective sample size proposed by Trenberth (1984) is used to minimize the influence of autocorrelation.

3. Temporal relationship

Figure 1(a) displays the annual frequencies of WNP TCs and RITCs during July–November from 1980–2021. Although TC and RITC frequencies are highly correlated ($r = 0.54$, $p < 0.01$), their spectra peak at different periods (figure 1(b), (c)). A period of 3–6 years dominate changes in TC frequency (figure 1(b)), which corresponds to the preferred timescale of ENSO. By comparison, RITC frequency exhibits a significant periodicity from 2–3 years (figure 1(c)), which is relatively shorter than the dominant period for TC frequency.

Figure 1(a) also displays the annual change of the WNPMI, which significantly correlates with both TC frequency ($r = 0.32$, $p = 0.04$) and RITC frequency ($r = 0.42$, $p < 0.01$). Choi *et al* (2016) reported a much higher correlation between the WNPMI and TC frequency ($r = 0.62$, $p < 0.01$), which possibly is a result of the different season analyzed (June–August). As shown in figure 1(d), similar to Li and Wang (2005), the WNPMI shows two preferred periods of 5–6 years and 2–3 years, which roughly correspond to the dominant periods of TC frequency and RITC frequency, respectively.

Furthermore, TC frequency and the WNPMI show significant coherence only on a timescale of 5–8 years (figure 1(e)). Comparatively, significant coherence between RITC frequency and the WNPMI is observed on a shorter timescale of 2–3 years. This means that although the WNP monsoon notably influences annual changes in both TC and RITC frequencies, its modulation peaks on distinct timescales. When focusing on biennial timescales, as displayed in table 1, the difference in the average TC frequency between strong and weak WNP monsoon years (2.6 TCs) is not statistically significant ($p = 0.08$). Accordingly, we suspect that the significant WNPMI-TC relationship found in Choi *et al* (2016) is primarily due to its relationship on longer than biennial timescales. By contrast, the average RITC frequency in strong WNP monsoon years is 2.7 TCs greater than that in weak WNP monsoon years. This difference is statistically significant ($p < 0.01$), confirming a notable WNP monsoon-RITC frequency linkage on the biennial timescale. Note that the TC frequency difference is comparable to the RITC frequency difference, while the differences in significance are mainly the result of the standard deviation of TC frequency (3.9 TCs) being much larger than that of RITC frequency (2.4 TCs).

4. Spatial relationship

Figure 2 displays differences in several TC-related metrics between the 13 strong WNP monsoon years and 14 weak WNP monsoon years. Choi *et al* (2016) reported that more TCs tended to form over the southeast (northwest) quadrant of the WNP during June–August during the positive (negative) phase of the WNPMI. By comparison, during July–November, the TC genesis difference between strong and weak WNP monsoon years exhibits an east-west dipolar pattern, with a boundary at around 135°E (figure 2(a)). During strong WNP monsoon years, unlike the dipolar pattern of June–August TC passage frequency differences shown in Choi *et al* (2016), there are higher TC track densities over almost the entire WNP during July–November (figure 2(b)). Because of enhanced TC genesis far away from the East Asian continent, more TCs experience recurving or northward-moving tracks. By contrast, there are only weak changes in TC track density east of 130°E, likely attributed to the offsetting of the following two factors. One is decreased TC genesis over the western WNP, which directly leads to suppressed TC activity over this region. The other is more TCs forming over the eastern WNP. Some of these TCs move straight westward or northwestward and subsequently enter the western WNP.

The spatial features of genesis (track density) differences for RITCs between strong and weak WNP monsoon years are quite similar to that for all TCs, with a pattern correlation coefficient of 0.86 (0.95) (figures 2(c), (d)). Enhanced TC activity is generally associated with enhanced RITC activity, since all TCs and RITCs share several common favorable environmental conditions (Wang and Zhou 2008). During strong WNP monsoon years, there are significantly more RITCs forming over the region of 5°–25°N, 140°–160°E (hereafter the key region), which only covers the eastern edge of the RI main development region (MDR; 10°–20°N, 125°–145°E; Song *et al* 2021) (figure 2(c)). During strong WNP monsoon years, more RITCs move westward across the MDR (figure 2(d)), where the climatological environment is most favorable for RI. Compared with TCs, RITCs take more westward-moving tracks and fewer northward-moving tracks during strong WNP monsoon years. TCs entering the MDR are more likely to undergo RI, while TCs entering higher-latitude regions are less likely to undergo RI. Moreover, during strong WNP monsoon years, there are notably more RI occurrences and greater RI ratios over the key region (figures 2(e), (f)). Note that the region with significantly enhanced RI occurrence is a little farther north of the region with significantly enhanced RITC genesis. These findings imply that some northward-moving RITCs experience RI quickly after genesis.

Figure 2 summarizes how RITC activity is influenced by the WNP monsoon. During strong WNP monsoon years, more TCs tend to form east of 135°E, particularly over the key region. Some of these TCs move westward into the MDR that climatologically has the most RI-favorable environmental conditions, These TCs subsequently have a great chance to experience RI. Other TCs undergo RI over the key region quickly after genesis, while moving northward towards higher latitudes. Both of these types of TCs can lead to an increase in RITC frequency during strong WNP monsoon years.

5. Environmental changes

Figure 3 shows differences in environmental conditions during July–November between strong and weak WNP monsoon years. Similar spatial structures are observed in differences of thermodynamic variables (e.g., SST, TCHP and 700–500-hPa relative humidity) (figures 3(a)–(c)). During strong WNP monsoon years, there are warmer waters, larger TCHPs and a moister atmosphere over the tropical central Pacific, while cooler waters, lower TCHPs and a drier atmosphere extend from the South China Sea (SCS) to the subtropical central Pacific. There are almost no significant SST and TCHP changes over the entire WNP, including over the key region (figures 3(a), (b)). However, significantly increased relative humidity is found in the zonal belt of 10°–20°N and east of 145°E (figure 3(c)).

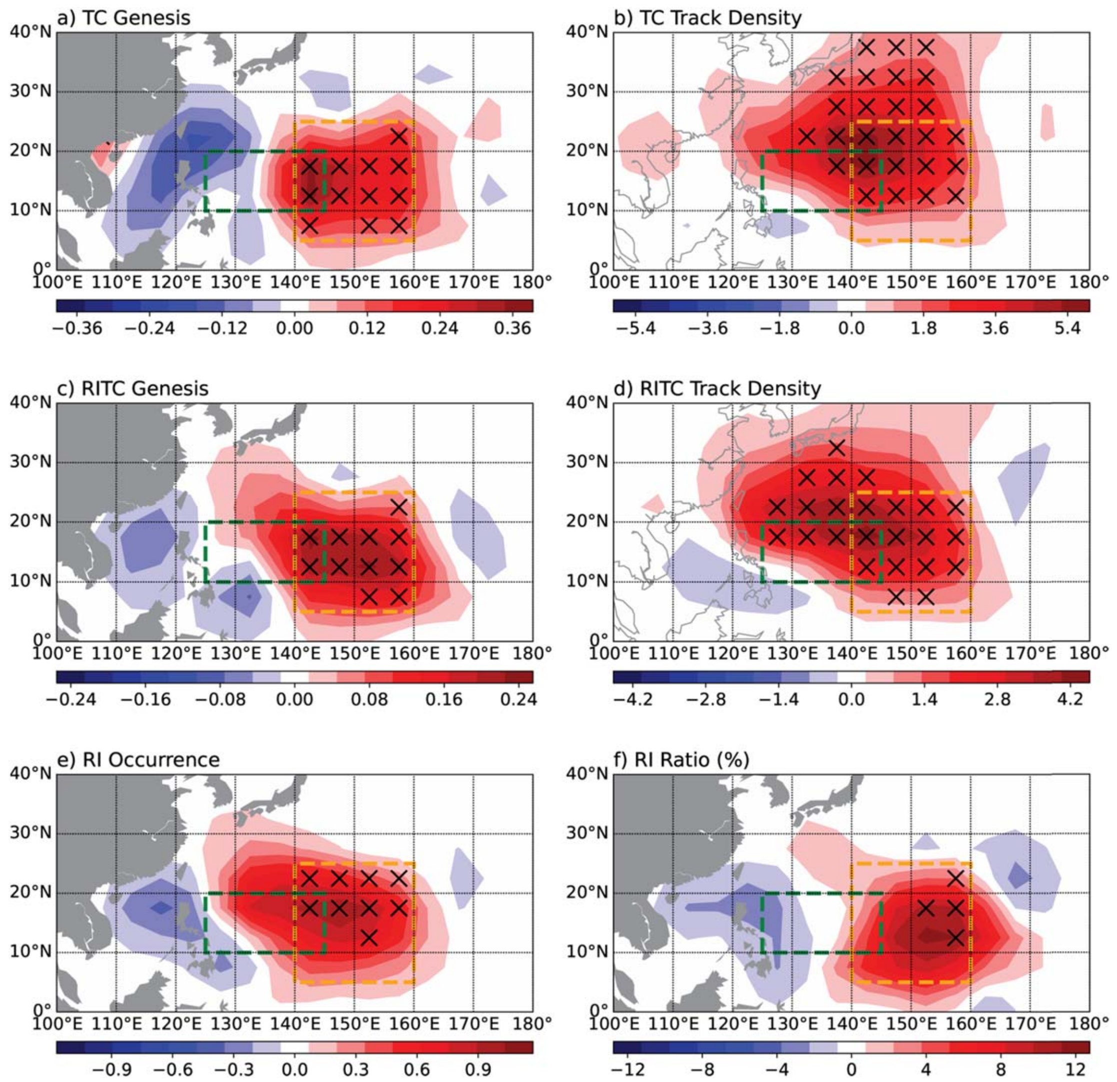

Figure 2. Differences in (a) TC genesis, (b) TC track density, (c) RITC genesis, (d) RITC track density, (e) RI occurrence and (f) RI ratio between strong and weak WNP monsoon years. Values are calculated over 5°×5° grids, while black crosses denote the differences significant at the 0.05 level based on a Student's *t*-test. Green dashed boxes indicate the main development region (MDR) for WNP RI events (10°–20°N, 125°–145°E), as identified in Song *et al* (2021). Yellow dashed boxes represent the key region, defined to be: 5°–25° N, 140°–160°E.

Differences in 850-hPa relative vorticity mainly show latitudinal differences (figure 3(d)). During strong WNP monsoon years, there is significantly increased relative vorticity between 10°–30°N and significantly decreased relative vorticity south of 10°N and north of 30°N. The difference in 200-hPa divergence has a similar spatial pattern to the vorticity difference (figure 3(e)), with a pattern correlation of 0.56 ($p < 0.01$). Over the region east of 120°E, there is increased (decreased) upper-level divergence south (north) of 25°N, roughly corresponding to increased (decreased) low-level vorticity. In addition, increased 850–200-hPa vertical wind shear is concentrated over the equatorial western WNP, while reduced vertical wind shear extends from the tropical central Pacific to the subtropical western WNP (figure 3(f)).

In summary, over the key region, SST and TCHP changes likely play only a minor role in modulating RITC activity between different WNP monsoon years (figures 3(a), (b)). In contrast, changes in atmospheric conditions primarily act to favor TC genesis and RI occurrence during strong WNP monsoon years compared with weak WNP monsoon years. These more favorable conditions during strong WNP monsoon years include increases in low-to-mid-level humidity, low-level vorticity and upper-level divergence and decreases in vertical wind shear (figures 3(c)–(f)). We note that when considering the biennial influence of the WNP monsoon, TC genesis and RI occurrence share similar preferred environments.

Figure 4 further shows how the WNP monsoon modulates changes in the aforementioned atmospheric conditions. Similar to Li and Wang (2005), a strong WNP monsoon is characterized by enhanced precipitation over the tropical WNP, with a suppressed convective region extending from Borneo to the North Indian Ocean (figure 4(a)). The only discrepancy between our study and Li and Wang (2005)'s study is over the SCS, where

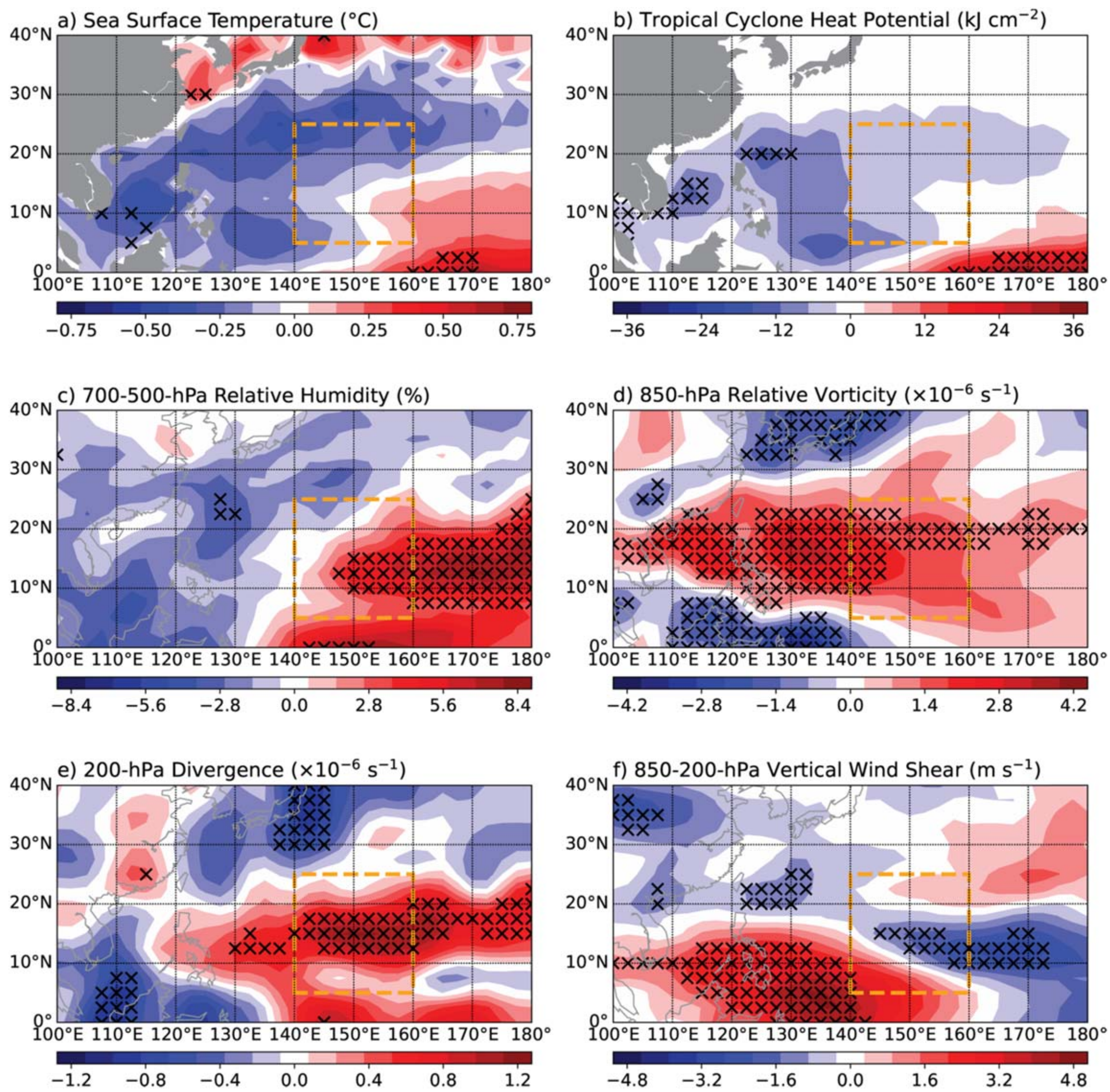

Figure 3. Differences in environmental variables between strong and weak WNP monsoon years, including (a) SST, (b) tropical cyclone heat potential, (c) 700–500-hPa relative humidity, (d) 850-hPa relative vorticity, (e) 200-hPa divergence, and (f) 850–200-hPa vertical wind shear. Differences significant at the 0.05 level based on a Student's *t*-test are displayed as black crosses on a 2.5°×2.5° grid. The yellow dashed boxes represent the key region of 5°–25°N, 140°–160°E.

increased and decreased rainfall was observed in Li and Wang (2005) and our study, respectively. This discrepancy may be due to the different seasons considered. Meanwhile, there is reduced precipitation over the mid-latitude regions of East Asia, indicating an opposite change of the WNP monsoon and the East Asian monsoon on biennial timescales.

Consistent with the precipitation difference over the WNP, during strong WNP monsoon years, there is an anomalous low-level cyclonic (anticyclonic) circulation south (north) of 30°N (figure 4(b)). This anomalous cyclone is centered over the key region, providing positive anomalous vorticity that is favorable for TC genesis and RI development. At 600 hPa, there are two anomalous cyclonic circulations over the tropical WNP, with the eastern part of the key region located between them (figure 4(c)). Over the eastern key region, there is moisture convergence due to northerlies to the east and southerlies to the west, leading to an increase in low-to-mid-level humidity. The anomalous circulation over the WNP at 200 hPa is nearly opposite to that at 850 hPa, exhibiting an anomalous anticyclone (cyclone) south (north) of 30°N (figure 4(d)). The key region is located near the center of the anticyclone, with associated upper-level divergence based on quasi-geostrophic theory. In addition, over the key region, anomalous westerlies (easterlies) oppose climatological easterlies (westerlies) at 850 hPa (200 hPa), indicating a slowdown of the environmental wind speed (figures 4(b), (d)). Given that the areal-averaged speed of the anomalous low-level westerlies (1.2 m s^{-1}) is much lower than that of the anomalous upper-level easterlies (3.3 m s^{-1}), the result is reduced vertical wind shear over the key region.

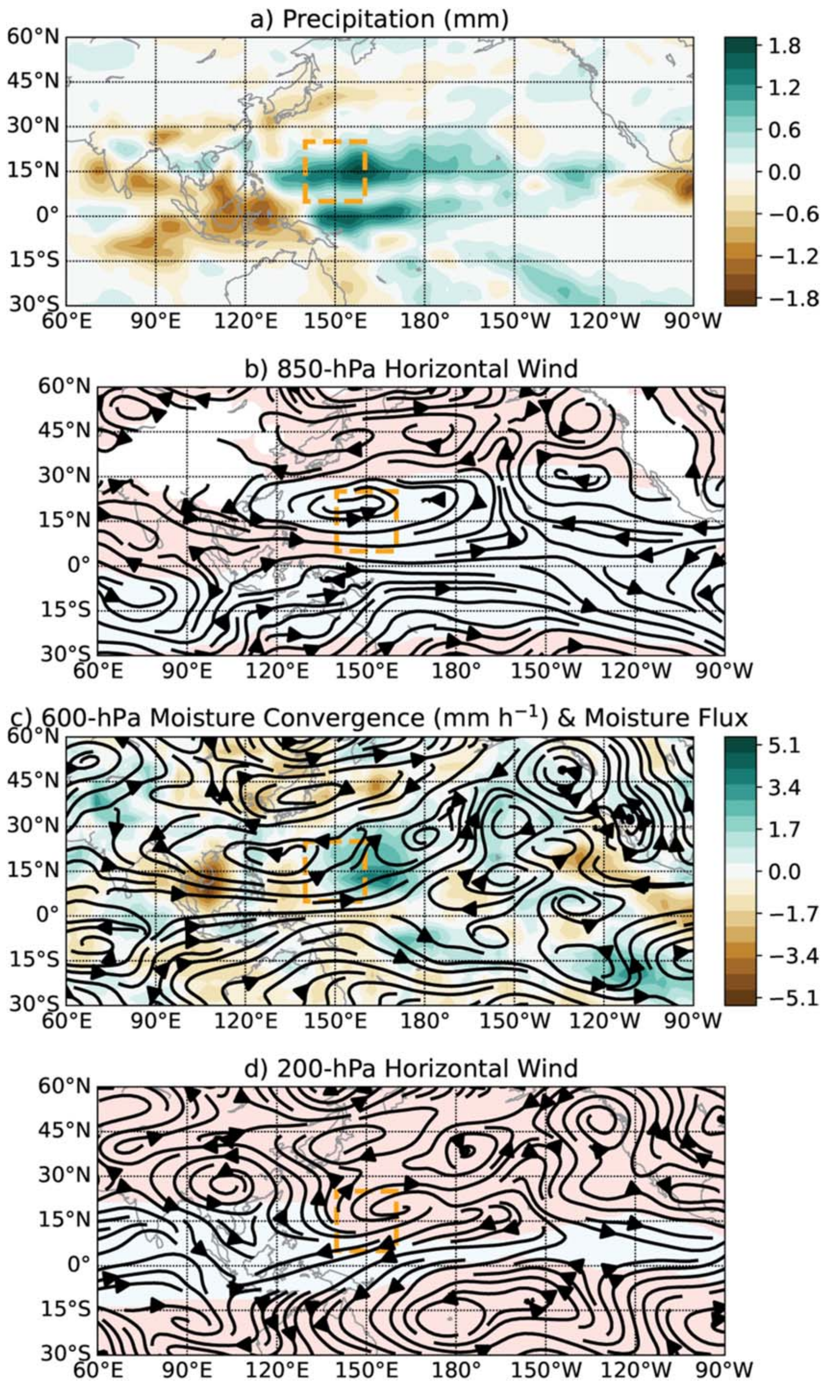

Figure 4. Differences in (a) precipitation, (b) 850-hPa horizontal wind, (c) 600-hPa moisture flux and convergence, and (d) 200-hPa horizontal wind between strong and weak WNP monsoon years. In (b) and (d), the regions with climatological westerlies and easterlies are colored in light red and light blue, respectively. The yellow dashed boxes represent the key region of 5°–25°N, 140°–160°E.

6. Conclusion

The modulation of WNP RITC activity by the WNP monsoon on biennial timescales is investigated in this study. There is a significant positive relationship between WNP RITC frequency during July–November and the simultaneous WNPMI, which primarily results from their correlation on biennial timescales. During strong monsoon years, there is enhanced TC genesis over the key region (5°–25°N, 140°–160°E). Some of these TCs move westward into the MDR which climatologically has the most RI-favorable environmental conditions. These TCs subsequently have a relatively high chance of undergoing RI. Other TCs undergo RI over the key region quickly after their genesis, while moving northward to higher latitudes. These both result in an increase in RITC frequency during strong WNP monsoon years.

The influence of the WNP monsoon on RITC activity can be explained by changes in large-scale environmental variables. In general, during strong WNP monsoon years, there is increased low-to-mid-level humidity, low-level vorticity and upper-level divergence and decreased vertical wind shear over the key region, which all favor TC genesis and RI development. Given the small observed changes in SST and TCHP, we find that atmospheric variable changes play a dominant role in influencing RITC activity over the WNP. Further analysis shows that a strong WNP monsoon is characterized by an anomalous 850-hPa cyclone and an anomalous 200-hPa anticyclone over the tropical WNP, providing positive vorticity and divergence at lower and upper levels, respectively. Over the key region, 600-hPa moisture convergence increases low-to-mid-level relative humidity, while 200-hPa wind has a larger decrease in magnitude than 850-hPa wind, reducing vertical wind shear.

Li and Wang (2005) concluded that the interannual variation of the WNP monsoon displayed two preferred timescales: one at low-frequency ENSO timescales (~4 years) and the other at quasi-biennial timescales. Our study highlights that the WNP monsoon significantly modulates TC and RITC frequency at distinct timescales. Our results are mainly obtained by statistical composite analysis. These results should be verified using numerical sensitivity tests. We intend to conduct these simulations in future work.

Acknowledgments

This work was funded by the National Natural Science Foundation of China (61827901, 42175007, 42192554 and 42192552). Klotzbach would like to acknowledge financial support from the G Unger Vetlesen Foundation.

Data availability statement

The data cannot be made publicly available upon publication because they are not available in a format that is sufficiently accessible or reusable by other researchers. The data that support the findings of this study are available upon reasonable request from the authors.

ORCID iDs

Jinjie Song https://orcid.org/0000-0003-3948-8894

References

Briegel L M and Frank W M 1997 Large-scale influences on tropical cyclogenesis in the western North Pacific *Mon. Wea. Rev.* **125** 1397–413
Cai Y, Han X, Zhao H, Klotzbach P J, Wu L, Raga G B and Wang C 2022 Enhanced predictability of rapidly intensifying tropical cyclones over the western north pacific associated with snow depth changes over the Tibetan plateau *J. Climate* **35** 2093–110
Chan J C L 2005 Interannual and interdecadal variations of tropical cyclone activity over the western North Pacific *Meteorol. Atmos. Phys.* **89** 143–52
Chen T –C, Wang S –Y, Yen M –C and Gallus W A Jr 2004 Role of the monsoon gyre in the interannual variation of tropical cyclone formation over the western North Pacific *Wea. Forecasting* **19** 776–85
Choi J –W, Kim B –J, Zhang R H, Park K –J, Kim J –Y, Cha Y and Nam J –C 2016 Possible relation of the western North Pacific monsoon to the tropical cyclone activity over western North Pacific *Int. J. Climatol.* **36** 3334–45
Daloz A S and Camargo S J 2018 Is the poleward migration of tropical cyclone maximum intensity associated with a poleward migration of tropical cyclone genesis? *Clim. Dyn.* **50** 705–15
DeMaria M, Franklin J L, Onderlinde M J and Kaplan J 2021 Operational forecasting of tropical cyclone rapid intensification at the National Hurricane Center *Atmosphere* **12** 683
Emanuel K A 2018 100 years of progress in tropical cyclone research *Meteor. Monogr.* **59** 15.1–15.68
Fudeyasu H, Ito K and Miyamoto Y 2018 Characteristics of tropical cyclone rapid intensification over the western North Pacific *J. Climate* **31** 8917–30
Galvin J F P 2014 The development, track and destruction of Typhoon Haiyan *Weather* **69** 307–9
Gao C, Zhou L, Wang C, Lin I –I and Murtugudde R 2022 Unexpected limitation of tropical cyclone genesis by subsurface tropical central-north Pacific during El Niño *Nat. Commun.* **13** 7746
Gao J, Zhao H, Klotzbach P J, Wang C, Raga G B and Chen S 2020 Possible influence of tropical indian ocean sea surface temperature on the proportion of rapidly intensifying western north pacific tropical cyclones during the extended boreal summer. *J. Climate* **33** 9129–43
Ge X, Shi D and Guan L 2018 Monthly variations of tropical cyclone rapid intensification ratio in the western North Pacific *Atmos. Sci. Lett.* **9** e814
Hersbach H *et al* 2020 The ERA5 global reanalysis *Quart. J. Roy. Meteor. Soc.* **146** 1999–2049
Kaplan J and DeMaria M 2003 Large-scale characteristics of rapidly intensifying tropical cyclones in the North Atlantic basin *Wea. Forecasting* **18** 1093–108
Kaplan J, DeMaria M and Knaff J A 2010 A revised tropical cyclone rapid intensification index for the atlantic and east pacific basins *Wea. Forecasting* **25** 220–41
Knaff J A, Sampson C R and Musgrave K D 2018 An operational rapid intensification prediction aid for the western North Pacific *Wea. Forecasting* **33** 799–811

Knapp K R, Kruk M C, Levinson D H, Diamond H J and Neumann C J 2010 The international best track archive for climate stewardship (IBTrACS) *Bull. Amer. Meteorol. Soc.* **91** 363–76
Lee C –Y, Tippett M K, Sobel A H and Camargo S J 2016 Rapid intensification and the bimodal distribution of tropical cyclone intensity *Nat. Commun.* **7** 10625
Li T and Wang B 2005 A review on the western North Pacific summer monsoon: synoptic-to-interannual variabilities *Terr. Atmos. Ocean Sci.* **16** 285–314
Li Y, Tang Y, Toumi R and Wang S 2022 Revisiting the definition of rapid intensification of tropical cyclones by clustering the initial intensity and inner-core size *J. Geophys. Res.* **127** e2022JD036870
Lin I –I, Black P, Price J F, Yang C –Y, Chen S S, Lien C –C, Harr P, Chi N –H, Wu C –C and D'Asaro E A 2013 An ocean coupling potential intensity index for tropical cyclones *Geophys. Res. Lett.* **40** 1878–82
Lin I –I *et al* 2020 ENSO and tropical cyclones ed M J McPhaden *et al El Niño Southern Oscillation in a Changing Climate.* (Washington, DC: American Geophysical Union) pp 377–408
Lin I –I, Chen C –H, Pun I –F, Liu W –T and Wu C –C 2009 Warm ocean anomaly, air sea fluxes, and the rapid intensification of tropical cyclone Nargis (2008) *Geophys. Res. Lett.* **36** L03817
Meehl G A 1987 The annual cycle and interannual variability in the tropical Pacific and Indian Ocean regions *Mon. Wea. Rev.* **115** 27–50
Meehl G A and Arblaster J M 2002 The Tropospheric Biennial Oscillation and Asian-Australian monsoon rainfall *J. Climate* **15** 722–44
Meehl G A, Arblaster J M and Loschnigg J 2003 Coupled ocean-atmosphere dynamical processes in the tropical Indian and Pacific oceans and the TBO *J. Climate* **16** 2138–58
Murakami T and Matsumoto J 1994 Summer monsoon over the Asian continent and western North Pacific *J. Meteor. Soc. Japan* **72** 719–45
Ritchie E A and Holland G J 1999 Large-scale patterns associated with tropical cyclogenesis in the western Pacific *Mon. Wea. Rev.* **127** 2027–43
Shi D, Ge X, Peng M and Li T 2020 Characterization of tropical cyclone rapid intensification under two types of El Niño events in the western North Pacific *Int. J. Climatol.* **40** 2359–72
Shu S, Ming J and Chi P 2012 Large-scale characteristics and probability of rapidly intensifying tropical cyclones in the western North Pacific basin *Wea. Forecasting* **27** 411–23
Song J, Klotzbach P J and Duan Y 2021 Increasing lifetime maximum intensity of rapidly intensifying tropical cyclones over the western North Pacific *Environ. Res. Lett.* **16** 034002
Tao S and Chen L 1987 A review of recent research on the East Asian summer monsoon in China *Monsoon Meteorology* ed C P Chang and T N Krishnamurti (Oxford, UK: Oxford University Press) pp 60–92
Taschetto A S and Ambrizzi T 2012 Can Indian Ocean SST anomalies influence South American rainfall? *Clim. Dyn.* **38** 1615–28
Trenberth K E 1984 Some effects of finite sample size and persistence on meteorological statistics *Part I: autocorrelations. Mon. Wea. Rev.* **112** 2359–68
Wang B and Fan Z 1999 Choice of south Asian summer monsoon indices *Bull. Amer. Meteor. Sci.* **80** 629–38
Wang B and Zhou X 2008 Climate variation and prediction of rapid intensification in tropical cyclones in the western North Pacific *Meteorol. Atmos. Phys.* **99** 1–16
Wang C, Deser C, Yu J –Y, DiNezio P and Clement A 2016 El Niño-Southern Oscillation (ENSO): a review *Coral Reefs of the Eastern Pacific* ed P Glymn *et al* (Dordrecht, The Netherlands: Springer Science Publisher) pp 85–106
Wu L, Wen Z, Huang R and Wu R 2012 Possible linkage between the monsoon trough variability and the tropical cyclone activity over the western North Pacific *Mon. Wea. Rev.* **140** 140–50
Zuo H, Balmaseda M A, Tietsche S, Mogensen K and Mayer M 2019 The ECMWF operational ensemble reanalysis-analysis system for ocean and sea-ice: a description of the system and assessment *Ocean Sci.* **15** 779–808